

# The environmental dependence of redox energetics of $\text{PuO}_2$ and $\alpha\text{-Pu}_2\text{O}_3$ : A quantitative solution from DFT+ $U$ calculations

Bo Sun\*, Haifeng Liu, Haifeng Song, Guang-Cai

Zhang, Hui Zheng, Xian-Geng Zhao, and Ping Zhang\*

*Institute of Applied Physics and Computational Mathematics, Beijing 100094, P.R. China*

## Abstract

We report a comprehensive density functional theory (DFT) +  $U$  study of the energetics of charged and neutral oxygen defects in both  $\text{PuO}_2$  and  $\alpha\text{-Pu}_2\text{O}_3$ , and present a quantitative determination of the equilibrium compositions of reduced  $\text{PuO}_2$  ( $\text{PuO}_{2-x}$ ) as functions of environmental temperature and partial pressure of oxygen, which shows fairly agreement with corresponding high-temperature experiments. Under ambient conditions, the endothermic reduction of  $\text{PuO}_2$  to  $\alpha\text{-Pu}_2\text{O}_3$  is found to be facilitated by accompanying volume expansion of  $\text{PuO}_{2-x}$  and the possible migration of O-vacancy, whereas further reduction of  $\alpha\text{-Pu}_2\text{O}_3$  is predicted to be much more difficult. In contrast to the endothermic oxidation of  $\text{PuO}_2$ , the oxidation of  $\alpha\text{-Pu}_2\text{O}_3$  is a stable exothermic process.

PACS numbers: 71.15.Nc, 61.72.Ji, 71.27.+a, 71.20.-b

---

\*Corresponding authors. Email addresses: sun\_bo@iapcm.ac.cn (B. Sun), zhang\_ping@iapcm.ac.cn (P. Zhang)

## I. INTRODUCTION

Plutonium oxides have long been of great interest not only for their high importance in nuclear fuel cycle and in long-term storage of Pu-based radioactive waste, but also their fancy physical properties and complex chemical reactions. Most of the rich behaviors of Pu ions in different oxidation states can be attributed to the complex character of Pu-5*f* orbitals[1–3], which locates in the boundary of localized and delocalized 5*f* states among the actinides. Since different oxidation states have widely different solubilities and demonstrate distinct effects on chemical corrosion of plutonium surface, the redox properties of Pu-oxides play a crucial role in the plutonium science and the reactor safety.

When exposed to oxygen-rich air, metallic Pu surface oxidizes readily to a protective dioxide (PuO<sub>2</sub>) layer[4–6], with a thin layer of the sesquioxide (Pu<sub>2</sub>O<sub>3</sub>) existing in between. Although, under special aqueous condition, the hydration reaction on PuO<sub>2</sub> surfaces (PuO<sub>2</sub> + *x*H<sub>2</sub>O → PuO<sub>2+*x*</sub> + *x*H<sub>2</sub>) has been reported to generate higher compound PuO<sub>2+*x*</sub> (*x* ≤ 0.27)[7], it has been theoretically proved to be strongly endothermic[8] and the products (PuO<sub>2+*x*</sub>) are experimentally found to be chemically unstable at elevated temperatures[9]. Thus, PuO<sub>2</sub> is the highest stable oxide as the compound of choice for the long-term storage of Pu. However, under oxygen-lean conditions (in the vacuum or inert gas), the PuO<sub>2</sub>-layer can be reduced to sesquioxides (Pu<sub>2</sub>O<sub>3</sub>), which can promote the hydrogenation of Pu metal[4, 10]. Besides the well-known sesquioxide β-Pu<sub>2</sub>O<sub>3</sub> in hexagonal structure (*P* $\bar{3}$ *m*1), the low-temperature sesquioxide phase is cubic α-Pu<sub>2</sub>O<sub>3</sub> (*Ia* $\bar{3}$ ), with ideal stoichiometric structure similar to the 2×2×2 fluorite PuO<sub>2</sub> (*Fm* $\bar{3}$ *m*) supercell containing 25% O vacancy located in the 16*c* (0.25, 0.25, 0.25) sites [see Fig. 1(top)]. In fact the cubic sesquioxide was detected in an abnormal body centered cubic PuO<sub>1.52</sub> form[11], since α-Pu<sub>2</sub>O<sub>3</sub> is stable only below 600 K and usually, a mixture of cubic PuO<sub>1.52</sub> and PuO<sub>1.98</sub> can be obtained by partial reduction of PuO<sub>2</sub> at high temperature and cooling to room temperature[12]. Meanwhile, the complex Pu-O phase diagram[13] shows that the PuO<sub>2</sub>-Pu<sub>2</sub>O<sub>3</sub> region mainly consists of widely nonstoichiometric compounds PuO<sub>2-*x*</sub> and has not been fully described since the nonstoichiometry can remarkably vary the properties of Pu oxides at high temperatures.

As the essential component of the uranium-plutonium mixed oxide (MOX) fuels in fast reactors, considerable efforts have been dedicated to the defect chemistry of Pu oxides[14–17], and theoretical models have been proposed based on the measured properties/parameters

such as the formation energy  $E^f$  of oxygen defects. More recently, Minamoto *et al.*[18] employed the DFT calculated  $E^f$  of single neutral O-vacancy to discuss the phase equilibrium of  $\text{PuO}_{2-x}$ - $\text{Pu}_2\text{O}_3$ , however, the conventional DFT that applies the local density approximation (LDA) or generalized gradient approximation (GGA) underestimates the strong correlation of the  $5f$  electrons and, consequently, describes  $\text{PuO}_2$  as incorrect ferromagnetic FM conductor [19] instead of antiferromagnetic AFM Mott insulator reported by experiment[20]. Fortunately, several beyond-DFT approaches, the DFT (LDA/GGA)+ $U$ [21], the self-interaction corrected LDA[2, 22], the hybrid density functional of (Heyd, Scuseria, and Enzerhof) HSE[23], and LDA + dynamical mean-field theory (DMFT)[24] have been developed to correct the failures of conventional DFT in calculations of Pu oxides. The effective modification of pure DFT by LDA/GGA+ $U$  formalisms has been confirmed widely in studies of  $\text{PuO}_2$ [27–35], which have reported the AFM-insulator ground state of  $\text{PuO}_2$ .

In this work, we present a comprehensive DFT+ $U$  study of the charge states and formation energies of oxygen point defects in both  $\text{PuO}_2$  and  $\alpha\text{-Pu}_2\text{O}_3$ , and the equilibrium compositions of  $\text{PuO}_{2-x}$  as functions of the environmental parameters (temperature and partial pressure of oxygen).

The rest of this paper is organized as follows. The details of our calculations are described in Sec. 2. In Sec. 3, we present and discuss the results. In Sec. 4, we summarize our main conclusions.

## II. DETAILS OF CALCULATION

The calculations are carried out using the Vienna *ab initio* simulation package[25] in the framework of the projector-augmented wave (PAW) method[26]. Following our previous DFT+ $U$  studies[27–32] of plutonium oxides, we apply the GGA+ $U$  scheme formulated by Dudarev *et al.*[21] to correct the strong on-site Coulomb repulsion among the Pu- $5f$  electrons. The choice of  $U$  and  $J$  parameters are based on an overall agreement between available experimental data and theoretical results as regarding the basic physical properties of  $\text{PuO}_2$  and  $\text{Pu}_2\text{O}_3$ , including the lattice constants, bulk modulus, phonon spectra and density of states (DOS), and the valence electronic DOS. Based on our extensive test calculations, it is found that the Hubbard  $U$  can alter the electronic-structure properties of  $\text{PuO}_2$  as well as

those of  $\alpha$ -Pu<sub>2</sub>O<sub>3</sub>. Specifically, when the effective parameter  $U_{eff}(=U-J)$  is less than 2.0 eV, the calculated electronic DOS indicates that  $\alpha$ -Pu<sub>2</sub>O<sub>3</sub> are metallic FM-conductor instead of the Mott-insulators. And the combination of  $U=4.75$  and  $J=0.75$  eV is proved to allow the ground-state properties of both PuO<sub>2</sub> and  $\alpha$ -Pu<sub>2</sub>O<sub>3</sub> to be reasonably described. A  $2\times 2\times 2$  supercell derived from the ideal fluorite PuO<sub>2</sub> is used, which accommodates 64 O and 32 Pu with the collinear **1k** AFM order. Following the recent DFT+ $U$  calculations of the ground state of **1k** AFM insulating UO<sub>2</sub>[36], we have carefully tested the use of such collinear **1k** AFM order to make the convergence to the ground state systematically, and strictly abided by the basic principle that the state with lowest total energy corresponds to the ground-state. The charged oxygen defects are modeled by adding or removing electrons from the supercell. The geometry optimization is carried out until the forces on all atoms are less than 0.01 eV/Å. The plane-wave cut-off energy of 400 eV and a  $7\times 7\times 7$  Monkhorst-Pack[37]  $k$ -point mesh (64 irreducible  $k$  points) are applied, and the convergences with respect to these input parameters are checked to be within 0.001 eV.

The formation energy of an isolated O-vacancy  $E_v^f$  or interstitial  $E_i^f$  in charge state  $q$  can be defined as

$$E_v^f = E_{vac} - E_{per} + \mu_O(T, p_{O_2}) + qE_F, \quad (1)$$

$$E_i^f = E_{int} - E_{per} - \mu_O(T, p_{O_2}) + qE_F, \quad (2)$$

where  $E_{vac}$ ,  $E_{int}$ , and  $E_{per}$  represent the total energies of the system with an O-vacancy, an O-interstitial, and the perfect system, respectively.  $E_F$  is the Fermi energy relative to the valence band maximum (VBM).  $\mu_O(T, p_{O_2})$  is the oxygen chemical potential under partial pressure  $p_{O_2}$ . Since the available experiments have just provided the related data [in Fig. 4(b)] under the conditions of such high temperature and particularly low pressure, where the interaction between the gaseous molecules is negligibly small, the ideal gas approximation of gaseous O<sub>2</sub> is expected to be reasonable. Thus, we can use the well-known thermodynamic expression[38]

$$\mu_O(T, p_{O_2}) = \frac{1}{2} (E_{O_2} + \tilde{\mu}_{O_2}(T, p^0) + k_B T \ln(p_{O_2}/p^0)), \quad (3)$$

where  $E_{O_2}$  is the total energy of the oxygen molecule. For the standard pressure  $p^0 = 1$  atm, the values of  $\tilde{\mu}_{O_2}(T, p^0)$  have been tabulated in Ref. [39]. With the “*ab initio* atomic

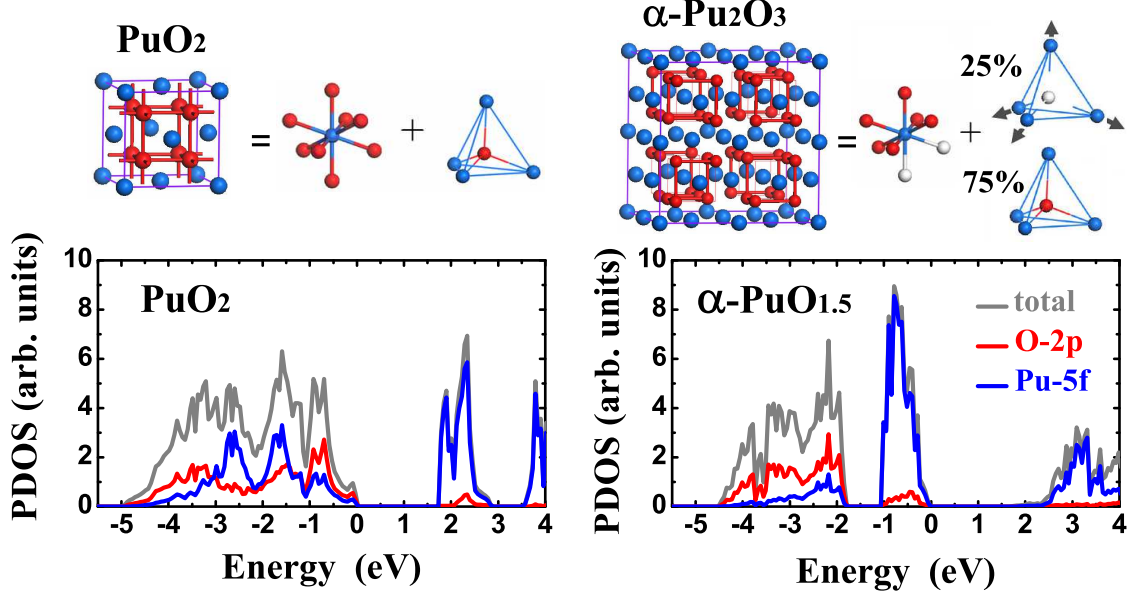


FIG. 1: (Color online) Top: crystal structures of  $\text{PuO}_2$  and  $\alpha\text{-Pu}_2\text{O}_3$  and their building blocks with grey arrows indicate the directions of the atomic displacements. The blue, red and white spheres denote the Pu, O atoms and O vacancies. Bottom: the atom-projected density of states (PDOSs) for Pu-5*f* and O-2*p* electrons in  $\text{PuO}_2$  (left) and  $\alpha\text{-Pu}_2\text{O}_3$  (right). The Fermi level is set to 0 eV.

thermodynamics” method[38], one can see that the zero-temperature DFT+*U* calculations just provide input parameters (total energies) for the thermodynamic formalism of the redox energetics [equations (1) and (2)], and the environmental dependence of  $E_v^f$  and  $E_i^f$  is therefore dominated by  $\mu_{\text{O}}$ , which includes three required and correlated factors, namely,  $T$ ,  $p_{\text{O}_2}$  and  $\tilde{\mu}_{\text{O}_2}$ . When compared to the experimental value of 2.56 eV[40], the DFT-GGA calculation is known to overestimate the binding energy of molecular  $\text{O}_2$  by 0.8 eV/0.5 $\text{O}_2$ [27, 41], and the correction term of 0.8 eV is thus applied in this work. The calculated oxidation reaction energies in  $\text{Pu}_2\text{O}_3 + \frac{1}{2}\text{O}_2 \rightarrow \text{PuO}_2$  are  $-3.81$  and  $-3.19$  eV for  $\beta\text{-Pu}_2\text{O}_3$  and  $\alpha\text{-Pu}_2\text{O}_3$ , respectively, which indicate that  $\alpha\text{-Pu}_2\text{O}_3$  is more stable at 0 K.

### III. RESULTS AND DISCUSSION

We begin by an overall comparison of the atomic- and electronic-structure properties between  $\text{PuO}_2$  and  $\alpha\text{-Pu}_2\text{O}_3$  presented in Fig. 1. In  $\text{PuO}_2$ , each Pu cation is bonded to eight O anions and every O is embedded in a regular Pu-cation tetrahedron, whereas after

an isostructure reduction to  $\alpha$ -Pu<sub>2</sub>O<sub>3</sub>, the coordination of Pu-cation reduces to six and O vacancies form in 25% Pu-tetrahedrons. The calculated lattice parameter  $a_0^{\alpha\text{-Pu}_2\text{O}_3}=1.120$  nm is close to the experimental values ranging from 1.103 to 1.107 nm[11, 12, 42], only a little larger than  $2a_0^{\text{PuO}_2}$  of 1.093 nm (in theory) and 1.079 nm (in experiment[7]), then an interesting volume expansion (7.6% in theory vs 7.4% in experiment) appears during the PuO<sub>2</sub>  $\rightarrow$   $\alpha$ -Pu<sub>2</sub>O<sub>3</sub> isostructure reduction. Moreover, in PuO<sub>2-x</sub>, the abnormal volume expansion is found to mount up almost linearly with the increasing nonstoichiometry  $x$  [see Fig. 4(a) below] in good agreement with experiments. The orbital-resolved atom-projected density of states (PDOS) suggests that the reason for such an abnormal issue is the localization of Pu-5*f* electrons after the formation of O-vacancy. Specifically, the highest occupied band (HOB) with a range of -5 to 0 eV is mainly the 5*f*(Pu)-2*p*(O) hybridization in PuO<sub>2</sub>. Whereas in  $\alpha$ -Pu<sub>2</sub>O<sub>3</sub>, the width of HOB decreases to 1.2 eV and the Pu-5*f* and O-2*p* occupied bands are well separated. The deduced populations of 5*f* state are 4.1 and 5.3 electrons in PuO<sub>2</sub> and  $\alpha$ -Pu<sub>2</sub>O<sub>3</sub>, respectively. Thus, the formation of O-vacancy in  $\alpha$ -Pu<sub>2</sub>O<sub>3</sub> or reduced PuO<sub>2</sub> withdraws 5*f* electrons from the bonding state and causes the coulomb repulsions among Pu cations with more localized 5*f* electrons. Both PuO<sub>2</sub> and  $\alpha$ -Pu<sub>2</sub>O<sub>3</sub> are insulators with the calculated gaps of 1.8 (the same as experiment[6]) and 2.0 eV.

For the isolated oxygen defects of different charge states in PuO<sub>2</sub> and  $\alpha$ -Pu<sub>2</sub>O<sub>3</sub>, the calculated zero-temperature  $E_v^f$  and  $E_i^f$  at the O-rich limit (i.e.  $p_{\text{O}_2}=p^0=1$  atm) as functions of the Fermi energy  $E_F$  in the insulating band gaps are shown in Fig. 2. Depending on the location of  $E_F$ , the thermodynamically stable charge states of O vacancies are found to vary between two values of +2 and 0 in PuO<sub>2</sub> [see Fig. 2(a)], and transit from +2 to 0 via +1 in  $\alpha$ -Pu<sub>2</sub>O<sub>3</sub> [Fig. 2(c)]. In both PuO<sub>2</sub> and  $\alpha$ -Pu<sub>2</sub>O<sub>3</sub>, it appears that the lowest  $E_v^f$  corresponds most of the time to the charge state of +2. And according to the signs and values of  $E_v^f$ , one can conclude that the reduction of PuO<sub>2</sub> (to  $\alpha$ -Pu<sub>2</sub>O<sub>3</sub>) is endothermic, and the further reduction of  $\alpha$ -Pu<sub>2</sub>O<sub>3</sub> will be much more difficult due to the much higher values of  $E_v^f$ . During the reduction of PuO<sub>2</sub> to nonstoichiometric PuO<sub>2-x</sub> compounds, the defect-chemistry study by Stan *et al.*[16] predicted that +2 O-vacancy is the dominating defect species at  $T = 1373$  K in the very low nonstoichiometry ( $x < 0.01$ ) region, namely, +2 O-vacancy dominates only at the beginning of the redox process, then +1 O-vacancy in a limited intermediate region, and finally neutral O-vacancy in the deep region ( $x \geq 0.025$ ). In current calculations based on a 2 $\times$ 2 $\times$ 2 PuO<sub>2</sub> supercell, the nonstoichiometry  $x$  is not

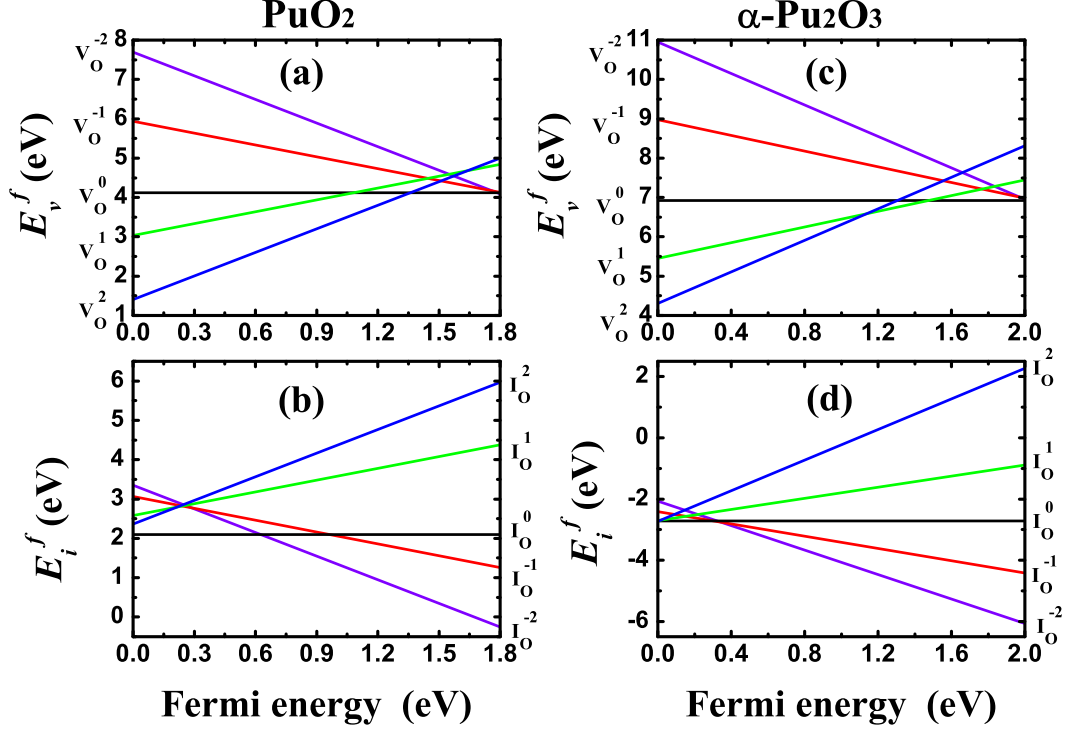


FIG. 2: (Color online) Formation energy  $E^f$  of oxygen point defects in different charge states as a function of Fermi energy in the band gap of  $\text{PuO}_2$  and  $\alpha\text{-Pu}_2\text{O}_3$ .

less than 0.03125 so that neutral O-vacancy will be the only dominating defect species according to the foregoing prediction. In both oxides, O interstitials can be  $-2$  or  $0$  charged depending on the position of  $E_F$ . In contrast to the endothermic oxidation of  $\text{PuO}_2$  (to higher oxides  $\text{PuO}_{2+x}$ ), a minus  $E_i^f$  indicates that the oxidation of  $\alpha\text{-Pu}_2\text{O}_3$  (to  $\text{PuO}_2$ ) is a stable exothermic process.

Assuming that both Pu-oxides are in equilibrium with an external environment and translating  $\mu_{\text{O}}$  into the environmental conditions ( $T$  and  $p_{\text{O}_2}$ ) according to Eq. (3), the results presented in Fig. 3(a)-(d) mainly show how a specific ideal gas approximation corrects the formation energies and influences the critical oxygen partial pressure  $p_{\text{O}_2}^c$  with  $E_v^f=0$  or  $E_i^f=0$  eV, namely, the evolutions of formation energies of neutral O defects as a function of  $T$  and  $p_{\text{O}_2}$ . The O point defects are found to be sensibly modulated by the environmental  $T$  and  $p_{\text{O}_2}$  as follows: (i) both  $E_v^f$  and  $E_i^f$  are independent of  $p_{\text{O}_2}$  when  $T = 0$  K; (ii) the  $E_v^f$  linearly decreases with decreasing  $\ln(p_{\text{O}_2})$  when  $T > 0$  K and reaches zero at a critical  $p_{\text{O}_2}^c$ , which increases with increasing temperature; (iii) the  $E_i^f$  linearly decreases with increasing

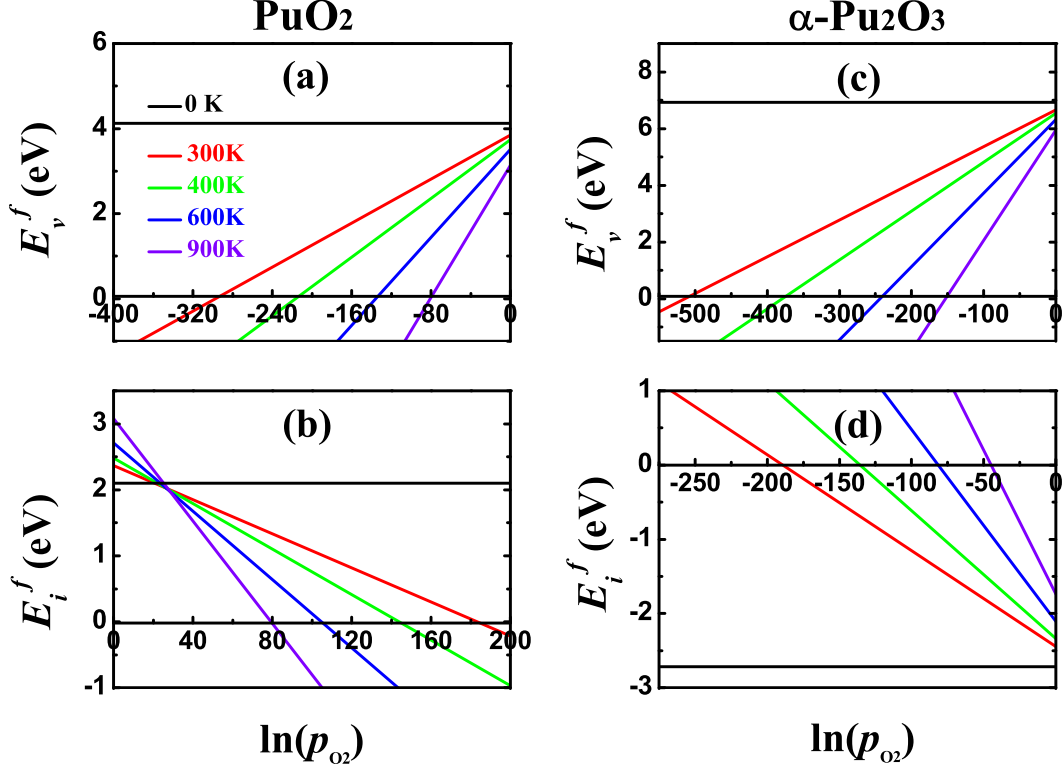


FIG. 3: (Color online) Dependence of the calculated formation energy of oxygen point defects in  $\text{PuO}_2$  and  $\alpha\text{-Pu}_2\text{O}_3$  on temperature  $T$  and oxygen partial pressures  $p_{\text{O}_2}$ .

$\ln(p_{\text{O}_2})$  when  $T > 0$  K and as  $T$  is increased, the critical  $p_{\text{O}_2}^c$  decreases for  $\text{PuO}_2$ , however increases due to the minus value of  $E_i^f$  for  $\alpha\text{-Pu}_2\text{O}_3$ ; (iv) when  $\ln(p_{\text{O}_2})=0$  (i.e.,  $p_{\text{O}_2}=p^0=1$  atm), under the ideal-gas approximation the  $\tilde{\mu}_{\text{O}_2}(T \neq 0, p^0)$  term can notably depress the  $E_v^f$  but increase  $E_i^f$  when compared with the corresponding formation energy at  $T = 0$  K, and it is particularly so at high temperatures. Thus, the  $\tilde{\mu}_{\text{O}_2}(T \neq 0, p^0)$  term is a contributory factor to figure out the critical  $p_{\text{O}_2}^c$  values, since it includes contributions from rotations and vibrations of molecular  $\text{O}_2$ , as well as the ideal-gas entropy at 1 atm.

Now we focus on the environment-dependent equilibrium compositions of nonstoichiometric  $\text{PuO}_{2-x}$ . The four points of  $p_{\text{O}_2}^c$  (at  $T=300, 400, 600$ , and  $900$  K) in Fig. 3(a), correspond to four environmental conditions, under which the  $\text{PuO}_{1.96875}$  compound is thermodynamically stable. For the further discussion of other  $\text{PuO}_{2-x}$  compounds, the averaged formation energy  $\bar{E}_v^f$  of neutral O-vacancy can be written as  $\bar{E}_v^f = \frac{1}{N_{\text{O-V}}} [E_{\text{vac}} - E_{\text{per}} + N_{\text{O-V}} \mu_{\text{O}}(T, p_{\text{O}_2})]$ , where  $N_{\text{O-V}}$  is the total number of O-vacancy in the  $\text{Pu}_{32}\text{O}_{64-N_{\text{O-V}}}$  supercell (with  $x = \frac{N_{\text{O-V}}}{32}$ ). According to the atomic structure of  $\alpha\text{-Pu}_2\text{O}_3$



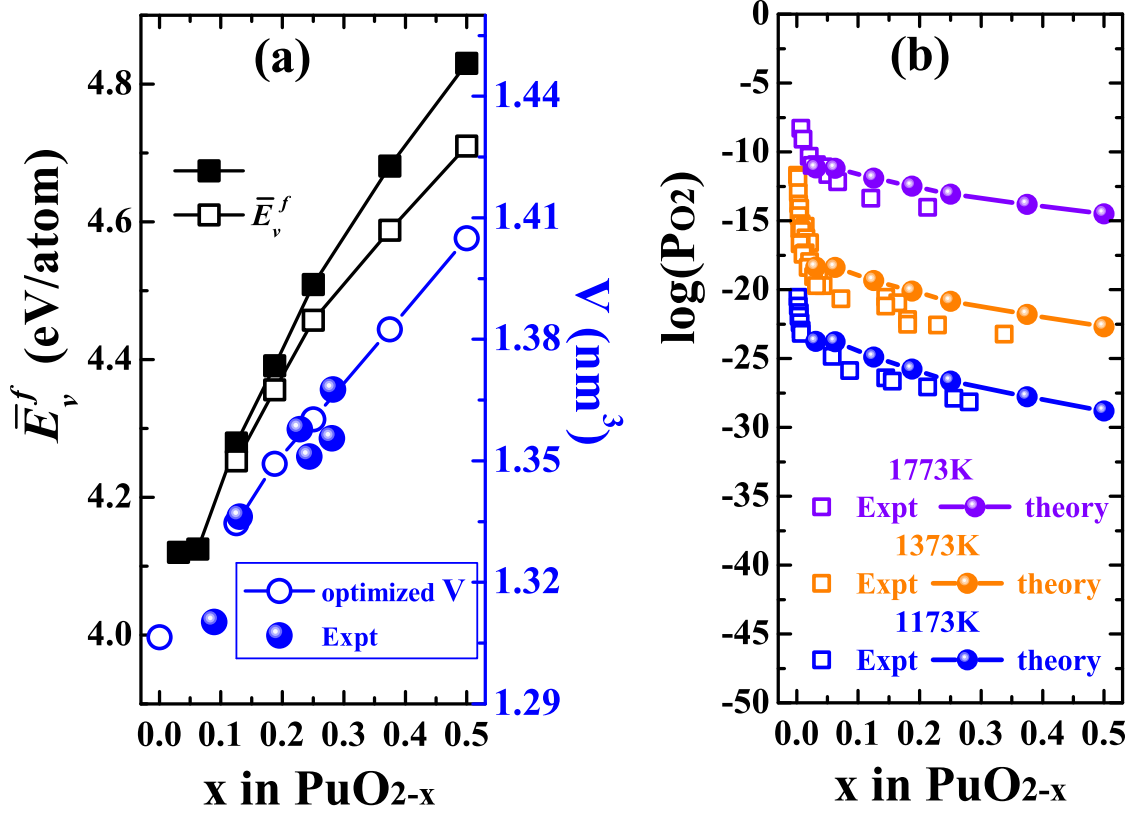


FIG. 4: (Color online) (a) The average formation energy  $\bar{E}_v^f$  of O-vacancy (left axis) and the optimized volume  $V$  of  $\text{PuO}_{2-x}$  (right axis) varies as the  $x$ . Solid and open squares -  $\bar{E}_v^f$  with and without volume optimization; Blue circles - optimized  $V$ ; Blue spheres - experimental  $V$  (compiled from Refs. [42] and [45]). (b) The calculated (spheres) and experimental (squares, compiled from Refs. [45–48]) relationships of equilibrium composition of  $\text{PuO}_{2-x}$  vs temperature and oxygen partial pressure. Lines are used to guide the eyes.

(see Fig. 1), we first adopt the  $\text{Pu}_{32}\text{O}_{64-N_{\text{O-V}}}$  supercell with even ( $N_{\text{O-V}} = 2, 4, 6, 8, 12$ , and 16) vacancies located along the parallel  $\langle 111 \rangle$  diagonals. In Fig. 4(a), the calculated  $\bar{E}_v^f$  (with and without volume optimization) and the optimized volume  $V$  of  $\text{Pu}_{32}\text{O}_{64-N_{\text{O-V}}}$ , together with the compiled experimental  $V$  of  $\text{PuO}_{2-x}$ , are plotted as functions of  $x$ . Although the volume expansion is found to effectively depress the  $\bar{E}_v^f$  when  $x \geq 0.25$ , the  $\bar{E}_v^f$  appears to monotonically increase with  $x$  and when  $x=0.5$  it reaches 4.71 eV, which is much larger than the reduction energy  $E^r$  of 3.19 eV in  $\text{PuO}_2 \Rightarrow \alpha\text{-Pu}_2\text{O}_3 + \frac{1}{2}\text{O}_2$ . This is due to the special and fully optimized distribution of O-vacancy in the stable  $\alpha\text{-Pu}_2\text{O}_3$ , specifically, vacancies located along four unequal and nonintersecting  $\langle 111 \rangle$  diagonals. We then partially

optimize the O-vacancy distribution based on the  $\text{Pu}_{32}\text{O}_{64-N_{\text{O-V}}}$  supercell with optimized  $V$  (for  $N_{\text{O-V}} = 4, 6, 8, 12$ ), and the corresponding  $\bar{E}_v^f$  is found to decrease with the increasing  $x$  and tend to approach  $E^r$  of 3.19 eV. To accomplish the optimum distribution, there may be many complex and correlated mechanisms and processes, among which the possible migration of O-vacancy and the accompanying volume expansion of the  $\text{PuO}_{2-x}$  matrix are doubtless very important and will be studied in our next work.

Figure 4(b) shows equilibrium compositions of  $\text{PuO}_{2-x}$  reported by this work as functions of environmental  $T$  and  $p_{\text{O}_2}$ , which appear to be in good agreement with experimental data at high temperatures of 1173 K, 1373 K and 1773 K. Thus, under special high-temperature and low-pressure conditions, the ideal-gas approximation is a reasonable enough request for a quantitative determination of the environment ( $T$  and  $p_{\text{O}_2}$ ) dependent phase equilibrium of  $\text{PuO}_{2-x}$ . As a comparison, since the  $\tilde{\mu}_{\text{O}_2}(T, p^0)$  term under the ideal-gas approximation is not considered, the equilibrium compositions of  $\text{CeO}_{2-x}$  and  $\text{HfO}_{2\pm x}$  reported by recent theoretical studies[43, 44] are found to be only qualitative agreement (instead of quantitative) with the corresponding high-temperature experiments. At low-temperature conditions, our results (not shown here) indicate that it is very hard to achieve the desired thermo-equilibrium conditions. However, with a reducing atmosphere such as CO or  $\text{H}_2$ , these conditions can be generated. Furthermore, in our DFT+ $U$  calculations, it is found that some cluster structures of O vacancies can efficiently decrease the average formation energy  $\bar{E}_v^f$ , the fact of which indicates that at low temperatures the optimized configuration of O vacancies in the  $\text{PuO}_{2-x}$  matrix is the actual key factor that influences the corresponding thermo-equilibrium conditions, whereas at high temperatures the O vacancies potentially have an even distribution.

#### IV. CONCLUSIONS

In summary, based on the DFT+ $U$  framework and the ideal-gas approximation, we systematically investigate the environmental dependence of the redox energetics of  $\text{PuO}_2$  and  $\alpha\text{-Pu}_2\text{O}_3$ . Our results clearly reveal that the reduction of  $\text{PuO}_2$  is an endothermic process, whereas the reduction of  $\alpha\text{-Pu}_2\text{O}_3$  will be much more difficult due to the higher formation energies of O-vacancy. In contrast to the endothermic oxidation of  $\text{PuO}_2$ , a minus formation energy of O-interstitial indicates that the oxidation of  $\alpha\text{-Pu}_2\text{O}_3$  is exothermic. And the re-

ported equilibrium compositions of  $\text{PuO}_{2-x}$  show quantitative agreement with experiments. Our current study may provide a guiding line to the understanding of redox behaviors of plutonium oxides.

## V. ACKNOWLEDGMENTS

This work was supported by the Foundations for Development of Science and Technology of China Academy of Engineering Physics under Grants No. 2010B0301048 and No. 2011A0301016.

- 
- [1] S. Y. Savrasov and G. Kotliar, Phys. Rev. Lett. 84 (2000) 3670.
  - [2] L. Petit, A. Svane, Z. Szotek, W. M. Temmerman, Science 301 (2003) 498.
  - [3] K. T. Moore and G. van der Laan, Rev. Mod. Phys. 81 (2009) 235.
  - [4] J. M. Haschke, Los Alamos Science 26 (2000) 253.
  - [5] M. T. Butterfield, T. Durakiewicz, I. D. Prodan, G. E. Scuseria, E. Guzewicz, J. A. Sordo, K. N. Kudin, R. L. Martin, J. J. Joyce, A. J. Arko, K. S. Graham, D. P. Moore, and L. A. Morales, Surf. Sci. 600 (2006) 1637.
  - [6] M. T. Butterfield, T. Durakiewicz, E. Guzewicz, J. Joyce, A. Arko, K. Graham, D. Moore, and L. Morales, Surf. Sci. 571 (2004) 74.
  - [7] J. M. Haschke, T. H. Allen, and L. A. Morales, Science 287 (2000) 285.
  - [8] P. A. Korzhavyi, L. Vitos, D. A. Andersson and B. Johansson, Nature Mater. 3 (2004) 225.
  - [9] T. Gouder, A. Seibert, L. Havela, and J. Rebizant, Surf. Sci. 601 (2007) L77.
  - [10] L. N. Dinh, J. M. Haschke, C. K. Saw, P. G. Allen, W. McLean II, J. Nucl. Mater. 408 (2011) 171.
  - [11] W. H. Zachariasen, Metallurgical Laboratory Report, CK-1530, 1944; T. D. Chikalla, C. E. McNeilly, R. E. Skavdahl, J. Nucl. Mater. 12 (1964) 131.
  - [12] IAEA technical reports series, No. 79, International Atomic Energy Agency, Vienna, 1967.
  - [13] H. A. Wriedt, Bull. All. Ph. Dia., 11(2) (1990) 184-202.
  - [14] T. M. Besmann and T. Lindemer, J. Nucl. Mater. 130 (1985) 489; *ibid.* 137 (1986) 292.
  - [15] A. Nakamura, J. Nucl. Mater. 201 (1993) 17.

- [16] M. Stan and P. Cristea, J. Nucl. Mater. 344 (2005) 213.
- [17] C. Guéneau, C. Chatillon, and B. Sundman, J. Nucl. Mater. 378 (2008) 257.
- [18] S. Minamoto, M. Kato, and K. Konashi, J. Nucl. Mater. 412 (2011) 338.
- [19] C. E. Boettger and A. K. Ray, Int. J. Quantum Chem. 90 (2002) 1470.
- [20] C. McNeilly, J. Nucl. Mater. 11 (1964) 53.
- [21] S. L. Dudarev, G. A. Botton, S. Y. Savrasov, C. J. Humphreys, and A. P. Sutton, Phys. Rev. B 57 (1998) 1505.
- [22] L. Petit, A. Svane, Z. Szotek, W. M. Temmerman, and G. M. Stocks, Phys. Rev. B 81 (2010) 045108.
- [23] I. D. Prodan, G. E. Scuseria, J. A. Sordo, K. N. Kudin, and R. L. Martin, J. Chem. Phys. 123 (2005) 014703.
- [24] Q. Yin and S. Y. Savrasov, Phys. Rev. Lett. 100 (2008) 225504.
- [25] G. Kresse and J. Furthmüller, Phys. Rev. B 54 (1996) 11169.
- [26] P. E. Blöchl, Phys. Rev. B 50 (1994) 17953.
- [27] B. Sun, P. Zhang, and X.-G. Zhao, J. Chem. Phys. 128 (2008) 084705.
- [28] B. Sun, and P. Zhang, Chin. Phys. B 18 (2008) 1364.
- [29] P. Zhang, B.-T. Wang, and X.-G. Zhao, Phys. Rev. B 82 (2010) 144110.
- [30] H. Shi, M. Chu, and P. Zhang, J. Nucl. Mater. 400 (2010) 151.
- [31] B. Sun, H. Liu, H. Song, G. Zhang, H. Zheng, X.-G. Zhao, and P. Zhang, J. Nucl. Mater. 426 (2012) 139.
- [32] H. Shi, and P. Zhang, J. Nucl. Mater. 420 (2012) 159.
- [33] D. A. Andersson, J. Lezama, B. P. Uberuaga, C. Deo, and S. D. Conradson, Phys. Rev. B 79 (2009) 024110.
- [34] G. Jomard, B. Amadon, F. Bottin, and M. Torrent, Phys. Rev. B 78 (2008) 075125.
- [35] G. Jomard, and F. Bottin, Phys. Rev. B 84 (2011) 195469.
- [36] B. Dorado, B. Amadon, M. Freyss, and M. Bertolus, Phys. Rev. B 79 (2009) 235125.
- [37] H. J. Monkhorst and J. D. Pack, Phys. Rev. B 13 (1976) 5188.
- [38] K. Reuter and M. Scheffler, Phys. Rev. B 65 (2001) 035406.
- [39] *NIST-JANAF Thermochemical Tables*, 4th ed., edited by J. Chase (American Chemical Society, Washington, DC, 1998).
- [40] K. P. Huber and G. Herzberg, *Molecular Spectra and Molecular Structure IV: Constants of*

*Diatomic Molecules* (Van Nostrand Reinhold, New York, 1979).

- [41] D. A. Andersson, S. I. Simak, B. Johansson, I. A. Abrikosov, and N. V. Skorodumova, Phys. Rev. B 75 (2007) 035109.
- [42] J. C. Boivineau, J. Nucl. Mater. 60 (1976) 31.
- [43] Y. Jiang, J. B. Adams, and M. Schilfgaarde, Appl. Phys. Lett. 87 (2005) 141917.
- [44] C. Tang and R. Ramprasad, Appl. Phys. Lett. 91 (2007) 022904.
- [45] T. L. Markin and M. H. Rand, Thermodynamics, vol. 1 (IAEA, Vienna, 1966) p. 145.
- [46] L. M. Atlas and G. J. Schlehman, in: A.E. Kay, M.B. Waldron (Eds.), Plutonium 1965, Chapman and Hall, London, 1965, p. 838.
- [47] G. C. Swanson, Los Alamos National Laboratory Report (LA-6063-T), 1975; R. E. Woodley, J. Nucl. Mater. 96 (1981) 5.
- [48] O. T. Sorensen, in: Proceedings of the Conference in Baden, 10C13 September 1975, North-Holland, Amsterdam, 1976.